

## Absence of dipole glass transition for randomly dilute classical Ising dipoles

Joseph Snider\* and Clare C. Yu

Department of Physics, University of California, Irvine, California 92697-4575, USA

(Received 13 September 2005; published 5 December 2005)

Dilute dipolar systems in three dimensions are expected to undergo a spin glass transition as the temperature decreases. Contrary to this, we find from Wang-Landau Monte Carlo simulations that at low concentrations  $x$ , dipoles randomly placed on a cubic lattice with dipolar interactions do not undergo a phase transition. We find that in the thermodynamic limit the “glass” transition temperature  $T_g$  goes to zero as  $1/\sqrt{N}$ , where  $N$  is the number of dipoles. The entropy per particle at low temperatures is larger for lower concentrations ( $x=4.5\%$ ) than for higher concentrations ( $x=20\%$ ).

DOI: [10.1103/PhysRevB.72.214203](https://doi.org/10.1103/PhysRevB.72.214203)

PACS number(s): 64.70.Pf, 75.10.Nr, 02.70.Uu, 75.40.Mg

Disordered insulating materials often have randomly placed electric or magnetic dipoles that have long-range dipolar interactions. Examples include impurities in alkali halides that can be used for paraelectric cooling,<sup>1,2</sup> diluted ferroelectric materials,<sup>3</sup> disordered magnetic materials, and frozen ferrofluids.<sup>4</sup> These systems are typically modeled with spin glass Hamiltonians that have simpler interactions and yet are believed to capture the essential physics of interacting dipoles. Based on theoretical studies of spin glasses with long-range interactions,<sup>5–8</sup> one would expect dilute Ising dipolar systems to undergo a spin glasslike transition as the temperature decreases. (We use the terms Ising and uniaxial synonymously.) In particular, the three-dimensional Ising spin glass with  $1/r^3$  interactions undergoes a finite temperature spin glass phase transition.<sup>8,9</sup> Since dipoles have similar interactions that fall off as  $1/r^3$ , one might expect disordered dipolar systems to also have a spin glass phase transition. However, in this paper we find the surprising result that, unlike such long-range spin glasses, dilute dipolar Ising systems do not undergo a spin glass phase transition as the temperature decreases. This may explain the lack of experimental evidence for such a transition in very dilute dipolar systems.

An example of dipoles is two-level systems (TLS) that dominate the physics of glasses at low temperatures.<sup>10</sup> TLS often have randomly oriented electric dipole moments that interact through an elastic strain field with a long-range interaction that is a stress tensor generalization of the vector dipolar interaction.<sup>11</sup> While there have been experimental hints of a spin glass transition among TLS in glasses at low temperatures,<sup>12</sup> there has been no definitive experimental proof that such a transition occurs. Since the estimated concentration of TLS is low (100 ppm), our result may explain the absence of a transition, even though TLS dipoles are randomly oriented and may not be uniaxial.

There are other examples of dilute dipolar systems that do not have finite temperature spin glass phase transitions. These include dilute  $\text{Eu}_x\text{Sr}_{1-x}\text{S}$ , where the  $\text{Eu}^{2+}$  ions have dipoles with  $s=7/2$  moments,<sup>13</sup> and a variety of Ising rubies [ $(\text{Cr}_x\text{Al}_{1-x})\text{O}_3$  with small  $x$ ].<sup>14</sup> Another example is the insulator  $\text{LiHo}_x\text{Y}_{1-x}\text{F}_4$  (Ref. 15) in which the holmium ions have Ising magnetic dipole moments that lie along the  $z$  axis due

to crystal field effects.<sup>16</sup> For very dilute systems ( $x=4.5\%$ )  $\text{LiHo}_x\text{Y}_{1-x}\text{F}_4$  shows no sign of a transition.<sup>17</sup> The lack of low-temperature freezing in  $\text{LiHo}_x\text{Y}_{1-x}\text{F}_4$  has been attributed to dominant quantum mechanical effects in the so-called spin liquid or antiglass phase.<sup>17,18</sup> However, a theoretical investigation of whether or not classical interacting dipoles undergo a spin glass phase transition at low concentrations has been lacking.

Several previous studies of dipolar interactions between randomly placed Ising dipoles have focused on the ferromagnetic transition that occurs at higher dipole concentrations.<sup>5,19,20</sup> Monte Carlo simulations have looked at intermediate concentrations with  $x \geq 25\%$ , where there is a spin glass transition.<sup>7,21</sup> Xu *et al.*<sup>6</sup> used mean field theory and found, depending on the lattice structure, ferromagnetic or antiferromagnetic transitions at higher concentrations. They found a spin glass phase at lower spin concentrations, but the properties of this phase were unreliable because they had a replica symmetric solution. In short, there have been no definitive theoretical studies of the very dilute classical cases. In this paper we present the results of Wang-Landau Monte Carlo simulations on classical dilute Ising dipolar systems in three dimensions. We find that there is no phase transition for low concentrations, in qualitative agreement with experiment.

In spin glasses the distribution  $P(q, T)$  of the overlap order parameter  $q$  changes from being a Gaussian centered at  $q=0$  at high temperatures to a bimodal distribution with peaks at  $q=\pm 1$  at low temperatures. At intermediate temperatures it is relatively flat. We can define a characteristic glass transition temperature  $T_g$  as the temperature where  $P(q, T)$  is the flattest. In the thermodynamic limit we find that for a given dipole concentration  $T_g$  goes to zero as  $1/\sqrt{N}$ , where  $N$  is the number of dipoles. Also, we examine the entropy and find that for concentrations less than 20% there is a nonzero entropy per dipole as  $T \rightarrow 0$ . The entropy and lack of a transition are consistent with a large number of accessible low-energy states and glassy behavior.

We consider Ising dipoles randomly placed on a simple cubic lattice at concentrations of  $x=4.5\%$ , 12%, and 20%. The interaction between any two dipoles  $\vec{p}_1$  and  $\vec{p}_2$  separated by a vector  $\vec{r}_{12}$  is given by the Hamiltonian

$$H(\vec{p}_1, \vec{p}_2) = \frac{\vec{p}_1 \cdot \vec{p}_2 - 3(\hat{r}_{12} \cdot \vec{p}_1)(\hat{r}_{12} \cdot \vec{p}_2)}{r_{12}^3}. \quad (1)$$

In addition to the energy units set by  $H$ , the units are set by  $\vec{p}_i = \pm \hat{z}$ , the lattice constant  $a=1$ , and Boltzmann's constant  $k_B=1$ . These will be referred to as MC units where appropriate. We use the Ewald summation technique to handle the long-range nature of the dipole interactions.<sup>22</sup> For  $x=4.5\%$ , the lattices had  $L^3$  sites with  $L=6, 8, 10$ , and  $12$ , and for  $x=12\%$  and  $20\%$ ,  $L=4, 6$ , and  $8$ . The number of dipoles  $N$  is the smallest even integer greater than or equal to  $xL^3$ .

The glassy energy landscape at low concentrations makes it difficult to equilibrate at low temperatures with the traditional Metropolis Monte Carlo approach. To overcome this, we have used the Wang-Landau (WL) Monte Carlo technique<sup>23</sup> to calculate the density of states  $n(E)$ , where  $E$  is the energy of the system. Briefly, this algorithm starts with an initial guess  $n(E)=1$  and executes a weighted random walk on the energy landscape. Single flips of randomly selected dipoles are then accepted with a probability of  $\min[1, n(E_i)/n(E_f)]$ , where  $E_i$  and  $E_f$  are the energies before and after the trial flip. If a step is accepted (rejected), then the density of states is updated by the rule  $n(E_{f(i)}) \rightarrow \gamma n(E_{f(i)})$ , where  $\gamma > 1$  is a scale factor. A histogram of the visited energies  $h(E)$  is recorded. The criterion for a satisfactory estimate of the density of states is given by the flatness of  $h(E)$ , i.e.,  $h(E) > \epsilon \langle h \rangle$  for every energy  $E$ , where  $\langle h \rangle$  is the average of  $h(E)$  and  $0 < \epsilon < 1$  determines the accuracy; typically,  $\epsilon \approx 0.95$ . Once the flatness condition is satisfied, the scale factor is set closer to 1 by the rule  $\gamma \rightarrow \sqrt{\gamma}$ ,  $h(E)$  is reset to zero, and the algorithm is repeated. In all cases, we ran 20 iterations with  $\gamma$  starting at  $e$  and ending at 1.000 001 9, and  $n(E)$  was normalized such that  $\sum_E n(E) = 2^N$ .

The dipolar interaction is nearly continuous so each energy bin may contain multiple states. We choose the bins to be as small as possible while maintaining reasonable computational times. The bin sizes depend on concentration and system size. The bins are about 0.01 in units of energy per particle for 20% filling and 0.001 for 4.5% and 12%. The lowest temperature studied ( $T=0.05$ ) must be larger than the largest bin (0.02). We try to keep the bins small enough so that  $n(E_0) \sim 2$ , where  $E_0$  is the energy of the (degenerate) ground state. In all cases except one,  $n(E_0) \approx 3.5$ . The exception ( $8^3$  at 20%) has  $n(E_0) \approx 10$ , so we discard the low-temperature values of this system.

We average over disorder by having different runs correspond to different quenched placements of dipoles with random initial orientations. The dipoles are fixed in position but not in orientation. There are about 1000 runs for each  $x$  and  $L$ . As a check of our Wang-Landau procedure, we were able to enumerate all the states for 1000 different configurations for concentrations of 4.5% ( $L=6$  and  $8$ ), 12% ( $L=4$ ), and 20% ( $L=4$ ) and determine the exact density of states. We found very good agreement with our WL results.

Since we are looking for a spin glass phase, we define a generalized Edwards-Anderson overlap order parameter  $q = 1/N \sum_i \vec{p}_i^s \cdot \vec{p}_i^s$ , where  $\vec{p}_i^s$  is a dipole in the state of the current system, and  $\vec{p}_i^s$  is a dipole in a low-energy state found in

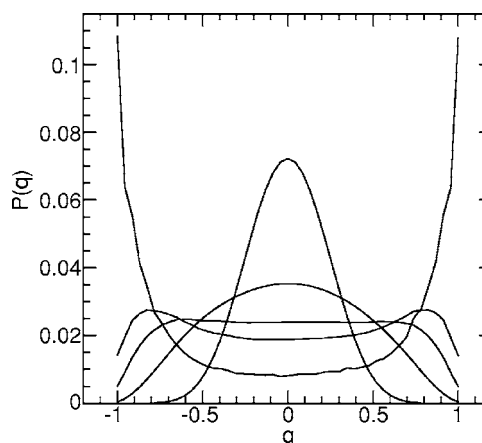


FIG. 1.  $P(q)$  at  $x=4.5\%$ ,  $L=10$  (46 dipoles).  $T=5, 1.6, 1.1, 0.9$ , and  $0.5$ . The lines transition from a Gaussian ( $T=5$ ) to a bimodal distribution ( $T=0.5$ ).

a short, initial simulation.<sup>24,25</sup> Then, to find the distribution  $P(q, E)$ ,  $q(E)$  is sampled and stored in a histogram during the simulation at the smallest scale factor where the estimate of the density of states is quite good.  $P(q, T)$  is calculated as

$$P(q, T) = C_T (1/Z) \sum_E n(E) P(q, E) \exp(-E/kT), \quad (2)$$

where the sum is over all the energy bins and  $Z(T) = \sum_E n(E) \exp(-E/kT)$ .  $C_T$  enforces normalization such that  $\sum_q P(q, T) = 1$  for every  $T$ . This method has been seen to give a reasonable order parameter distribution in the case of a Potts model.<sup>25</sup>

It has often been convenient to find the spin glass transition temperature using Binder's  $g = [3 - \langle (q^4) / \langle q^2 \rangle^2] / 2$ , and  $\langle q^m \rangle = \sum_q q^m P(q, T)$ .<sup>26</sup> Since the ground state estimate is not the true ground state, we eliminate all runs in which  $g < 0.8$  at the lowest temperature. If there is a second-order phase transition, plots of  $g$  vs  $T$  for different size systems will cross at the transition temperature.<sup>24</sup> However, we find that these curves do not cross, so there is no second-order spin glass phase transition.

To investigate this further, we can look at how  $P(q, T)$  changes with temperature. For a system undergoing a phase transition, we expect  $P(q, T)$  to change from being a Gaussian centered at  $q=0$  at high temperatures to a bimodal distribution with peaks at  $q=\pm 1$  at low temperatures. A typical example is shown in Fig. 1 for  $x=4.5\%$ ,  $L=10$ . We define a characteristic "glass" temperature  $T_g$  as the temperature where the distribution  $P(q, T)$  is flattest. We define the deviation  $D(T)$  from flatness in terms of the variance of  $P(q, T)$  as

$$D(T) = L^3 \langle (P(q, T) - \langle P(q', T) \rangle_{q'})^2 \rangle_q, \quad (3)$$

where  $\langle \dots \rangle_q$  indicates an average over all  $N+1$  possible values of  $q$ .  $D(T)$  is at a minimum when a plot of  $P(q, T)$  vs  $q$  is the flattest, defining  $T_g$ .  $D(T)$  is plotted in Fig. 2. For a given dilute concentration,  $T_g$  is tending to smaller temperatures as the system size increases which is consistent with  $T_g \rightarrow 0$  as  $L \rightarrow \infty$ . To find the dependence of  $T_g$  on the number

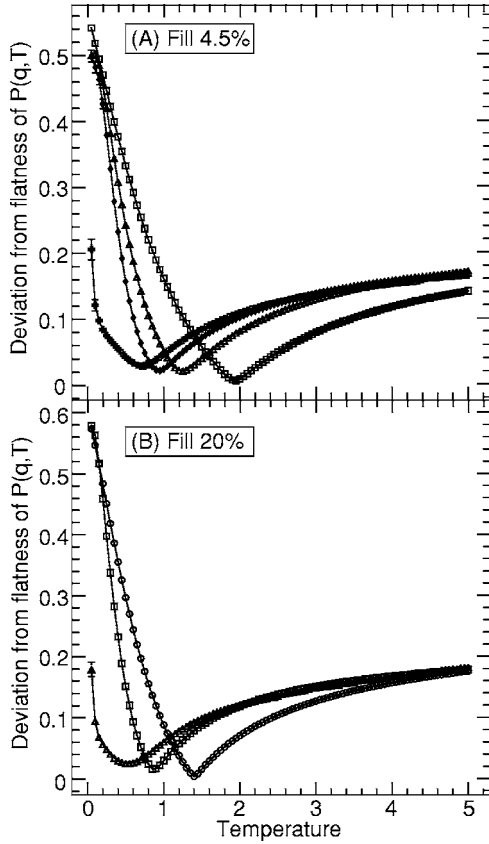


FIG. 2. The deviation from flatness for  $P(q, T)$ . Part A shows the results for  $x=4.5\%$  with sizes  $L=6, 8, 10,$  and  $12$ . Part B shows results for  $x=20\%$  with sizes  $L=4, 6,$  and  $8$ . In both cases the minima moves left with increasing size. The dip defines a glass transition temperature. The minima are more rounded as the system size increases because the transition is going away.

$N$  of dipoles for a fixed concentration, we plot the minimum of  $D(T)$  vs  $N$  in Fig. 3. The best fit for dilute cases reveals that  $T_g \sim N^{-1/2}$ . In contrast,  $D(T)$  for the ordered case ( $x=100\%$ ) yields a nonzero transition temperature, independent of  $N$ .

The absence of a transition is consistent with the experimental finding that for very dilute systems ( $x=4.5\%$ )  $\text{LiHo}_x\text{Y}_{1-x}\text{F}_4$  shows no sign of a transition.<sup>17</sup> However, the absence of a transition in dilute dipolar systems is unexpected since three-dimensional (3D) Ising spin glasses with  $1/r^3$  interactions undergo a phase transition.<sup>8,9</sup>  $P(q)$  for a spin glass and for a dilute dipolar system are different; in the thermodynamic limit as  $T \rightarrow 0$ ,  $P(q)$  for a spin glass has a few sharp peaks corresponding to ground state configurations separated by high barriers, while  $P(q)$  for the dilute dipolar system is flat, indicating numerous accessible low-energy states separated by insignificant barriers. With very low barriers, states at both the top and bottom of the barrier contribute low-energy states. The difference in barrier heights may be due to every site in a model spin glass being occupied so that in a spin glass with power law interactions nearby spins will tend to have stronger interactions than distant spins and produce large barrier heights. In a dilute dipole system nearby sites are empty and so the low-energy configurations

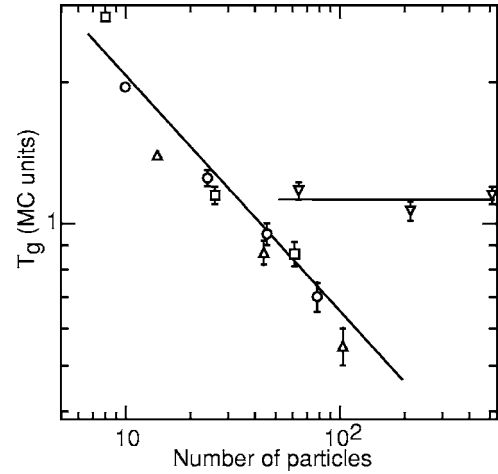


FIG. 3. Log-log plot of the maximum flatness for  $P(q)$  versus the number of dipoles at various concentrations. Open circles are 4.5%, squares are 12%, triangles are 20%, and upside down triangles are 100%. The left solid line has a slope of  $-1/2$  corresponding to  $T_g \sim N^{-1/2}$ . The right solid line has a slope of zero. Fits to  $T_g \sim N^{-\alpha}$  yield  $\alpha=0.49(1)$  for 4.5%,  $\alpha=0.6(1)$  for 12%,  $\alpha=0.45(3)$  for 20%, and  $\alpha=0.02(5)$  for 100%. The errors in the last digit are in parentheses.

are determined by distant dipoles that interact weakly and produce low barriers.

The presence of many nearly degenerate accessible ground states is reflected in the finite entropy per dipole near  $T=0$ . We find that the low-temperature entropy is larger for the lower concentration. We can calculate the total entropy  $S_{tot}(T)$  directly from the density of states obtained by our WL Monte Carlo simulations:

$$S_{tot}(T) = \frac{\langle E(T) \rangle}{T} + \log Z(T), \quad (4)$$

where  $\langle E(T) \rangle$  is the average energy of the system.  $S_{tot}$  is an absolute entropy and is not defined relative to some reference value. To compare different system sizes, we consider the entropy per particle  $S_N = S_{tot}/N$ , where  $N$  is the number of dipoles. The entropy is very smooth, corresponding to a broad bump in the specific heat.

To determine the entropy in the thermodynamic limit, we plot  $S_N(T)$  vs  $1/N$  at a given temperature  $T$ . We fit a line to the data and then extrapolate to  $N \rightarrow \infty$ . Then, we plot the extrapolated value versus temperature (see Fig. 4). From Figure 4, it is clear that the 4.5% and 12% cases have a nonzero entropy at low temperatures, but the 20% case is approaching zero. Finally, the extrapolated values are fit with a power law of the form  $AT^\lambda + S_0$ , where  $A$  and  $\lambda$  are constants, and  $S_0$  is a constant representing the zero temperature value of the entropy. The fit values are  $A=1.1 \pm 0.2$ ,  $\lambda=2.7 \pm 0.1$ , and  $S_0=(7.9 \pm 0.3) \times 10^{-3}$  at 4.5%,  $A=1.2 \pm 0.3$ ,  $\lambda=2.9 \pm 0.2$  and  $S_0=(5.6 \pm 0.3) \times 10^{-3}$  at 12%, and  $A=0.37 \pm 0.05$ ,  $\lambda=1.9 \pm 0.1$  and  $S_0=(-0.5 \pm 0.5) \times 10^{-3}$  at 20%. Note that the extrapolation at 20% gives a negative  $S_0$ , so it is zero; no actual data points have negative entropy. A phase diagram of the entropies at zero temperature is constructed in the inset of

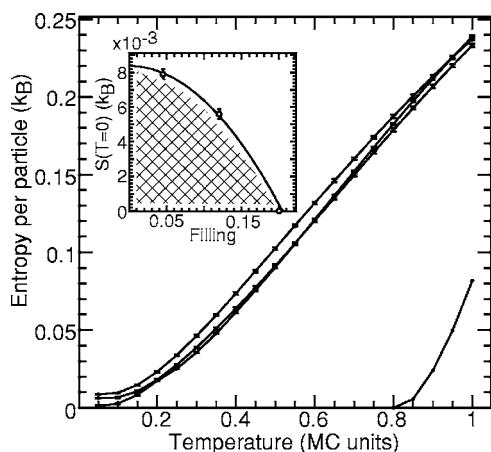


FIG. 4. Entropy per particle extrapolated to infinite size. From top to bottom the fillings are 4.5%, 12%, and 20%. The curve on the far right is for 100%. The error bars shown represent the standard error ( $\sim 10^{-3}$ ) of the distribution of  $S(T)$ . Inset: Entropy at  $T=0$  phase diagram. The hashed area is classically not accessible. The solid line is a guide to the eye. Above 20%,  $S(T=0)$  is zero.

Fig. 4. Notice that the low-temperature entropy increases as the concentration decreases. This indicates that there are more accessible low-energy states in systems with lower concentrations where the dipoles interact more weakly. Hav-

ing a finite value of  $S_0$  implies that the zero temperature entropy  $S(0)$  may be nonzero, but this is not unprecedented for a classical system, e.g., noninteracting spins.

We do not think that the finite entropy near  $T=0$  is due to the finite size of the energy bins. To test the effect of the bin size, we halved the bin size (doubled the number of bins) for the case of  $6^3$  at 20% and found an entropy change of about 5%, which is consistent with the error estimates. We also ran the largest exact case ( $8^3$  at 4.5%) through the WL algorithm with bins of width 0.005, and found a change of 0.9% compared to the exact result with zero bin width.

To summarize, we find the surprising result that at low concentrations ( $x \leq 20\%$ ) there is no spin glass-like phase transition as the temperature is lowered. This is consistent with having a large number of nearly degenerate accessible low-energy states. Our result could explain the lack of experimental evidence for a transition in dilute dipolar systems such as  $\text{LiHo}_x\text{Y}_{1-x}\text{F}_4$  for small  $x$  and among two-level systems in glasses at low temperatures. Thus, contrary to widely held notions, materials with dilute electric or magnetic dipoles cannot necessarily be modeled with spin glass Hamiltonians with long-range interactions.

We thank Stuart Trugman and Manoranjan Singh for helpful discussions. This work was supported by DOE Grants No. DE-FG03-00ER45843 and No. DE-FG02-04ER46107.

\*Present address: The Salk Institute, La Jolla, CA 92037.

- <sup>1</sup>W. Känzig, J. H. R. Hart, and S. Roberts, Phys. Rev. Lett. **13**, 543 (1964).
- <sup>2</sup>V. Narayanamurti and R. O. Pohl, Rev. Mod. Phys. **42**, 201 (1970).
- <sup>3</sup>B. E. Vugmeister and M. D. Glinchuk, Rev. Mod. Phys. **62**, 993 (1990), and references therein.
- <sup>4</sup>W. Luo, S. R. Nagel, T. F. Rosenbaum, and R. E. Rosensweig, Phys. Rev. Lett. **67**, 2721 (1991).
- <sup>5</sup>M. J. Stephen and A. Aharony, J. Phys. C **14**, 1665 (1981).
- <sup>6</sup>H.-J. Xu, B. Bergersen, F. Niedermayer, and Z. Rácz, J. Phys.: Condens. Matter **3**, 4999 (1991).
- <sup>7</sup>C. C. Yu, Phys. Rev. Lett. **69**, 2787 (1992).
- <sup>8</sup>H. G. Katzgraber and A. P. Young, Phys. Rev. B **67**, 134410 (2003).
- <sup>9</sup>A. J. Bray, M. A. Moore, and A. P. Young, Phys. Rev. Lett. **56**, 2641 (1986).
- <sup>10</sup>P. Esquinazi, *Tunneling Systems in Amorphous and Crystalline Solids* (Springer-Verlag, Berlin, 1998).
- <sup>11</sup>C. C. Yu, Phys. Rev. Lett. **63**, 1160 (1989).
- <sup>12</sup>P. Strehlow, C. Enns, and S. Hunklinger, Phys. Rev. Lett. **80**, 5361 (1998).

- <sup>13</sup>J. Kötzler and G. Eisel, Phys. Rev. B **25**, 3207 (1982).
- <sup>14</sup>J. Kötzler, G. Hesse, H. P. Tödter, and G. Eisel, Z. Phys. B: Condens. Matter **68**, 451 (1987).
- <sup>15</sup>D. H. Reich, B. Ellman, J. Yang, T. F. Rosenbaum, G. Aeppli, and D. P. Belanger, Phys. Rev. B **42**, 4631 (1990).
- <sup>16</sup>P. E. Hansen, T. Johansson, and R. Nevald, Phys. Rev. B **12**, 5315 (1975).
- <sup>17</sup>S. Ghosh, R. Parthasarathy, T. F. Rosenbaum, and G. Aeppli, Science **296**, 2195 (2002).
- <sup>18</sup>S. Ghosh, T. F. Rosenbaum, G. Aeppli, and S. N. Coppersmith, Nature **425**, 48 (2003).
- <sup>19</sup>H. Zhang and M. Widom, Phys. Rev. B **51**, 8951 (1995).
- <sup>20</sup>G. Ayton, M. J. P. Gingras, and G. N. Patey, Phys. Rev. E **56**, 562 (1997).
- <sup>21</sup>S. J. K. Jensen and K. Kjaer, J. Phys.: Condens. Matter **1**, 2361 (1989).
- <sup>22</sup>S. W. deLeeuw, J. W. Perram, and E. R. Smith, Proc. R. Soc. London, Ser. A **373**, 27 (1980).
- <sup>23</sup>F. Wang and D. P. Landau, Phys. Rev. E **64**, 056101 (2001).
- <sup>24</sup>R. N. Bhatt and A. P. Young, Phys. Rev. B **37**, 5606 (1988).
- <sup>25</sup>C. Yamaguchi and Y. Okabe, J. Phys. A **34**, 8781 (2001).
- <sup>26</sup>K. Binder, Z. Phys. B: Condens. Matter **43**, 119 (1981).